Surface & Coatings Technology 204 (2010) 1229–1235

Contents lists available at ScienceDirect

Surface & Coatings Technology

journal homepage: www.elsevier.com/locate/surfcoat

Effect of SiO_2:Na_2O molar ratio of sodium silicate on the corrosion resistance of silicate conversion coatings

Mei-rong Yuan, Jin-tang Lu, Gang Kong *

School of Material Science and Engineering, South China University of Technology, Wushan Road, 510640-Guangzhou, China

ARTICLE INFO

Article history:
Received 31 May 2009
Accepted in revised form 12 October 2009
Available online 20 October 2009

PACS:
68.55.-a
81.70-Jb
82.45.Bb

Keywords:
Hot-dip galvanized
Silicate coatings
Corrosion
Morphology

ABSTRACT

Passivation treatment by sodium silicate solution is considered as an alternative to chromium chemical conversion treatment to improve the corrosion resistance of hot-dip galvanized (HDG) steels. In this paper, a transparent silicate coating was formed on the surface of HDG steel by immersing in sodium silicate solution with SiO_2:Na_2O molar ratio in the range from 1.00 to 4.00. The parameter about the SiO_2:Na_2O molar ratio of silicate solution has been discussed using corrosion resistance and surface morphology. Tafel polarization, electrochemical impedance spectroscopy (EIS) measurements and neutral salt spray (NSS) test show that silicate coatings increase the corrosion resistance of HDG steels. From the results obtained, it is deduced that the optimum SiO_2:Na_2O molar ratio is 3.50. Scanning electron microscopy (SEM), X-ray photoelectron spectroscopy (XPS), X-ray diffraction analysis (XRD), and reflectance absorption infrared spectroscopy (RA-IR) show that there are no obvious differences of the chemical composition and structure in various silicate coatings. The silicate coatings mainly consist of zinc oxides/hydroxides, zinc silicate and SiO_2. However, atomic force microscopy (AFM) images reveal that the surface of silicate coatings with a molar ratio of 3.50 is more compact and uniform than other silicate coatings.

1. Introduction

Hot-dip galvanizing (HDG) steels have many useful properties that are suitable for widely applications such as automobiles, architectures, transportation and housewares. However, the dissolution rate of Zn is high due to the large potential difference between the steel substrate and zinc layer [1]. Among many corrosion protection methods, passivation post treatment is a very important method. As it is well known, chromate coatings are the most effective coatings for HDG steels due to their self-healing nature and corrosion resistance properties. Due to the high-toxic and carcinogenic hexavalent chromium salts, passivation treatments from Cr(VI) may be banned by the Environmental Protection Agency (EPA) [2]. Hence, there is a great need to develop an environmentally friendly coating to replace the chromate coating.

In recent years, many attempts have been made to find alternatives, such as inorganic salts—molybdate [3,4], tungstate [5], rare earth salt [6], silicate [7] or organic compounds—epoxy resin [8,9], acrylate [10], and silane [11,12].

It is well known that sodium silicate is an effective corrosion inhibitor and has been used as a corrosion inhibitor for years [13]. Recently, the deposition of thin silicate coatings on galvanized steels [1,7,13–16], aluminum and alloys [17], and magnesium alloys [18] have been extensively investigated. It can be achieved from single sodium silicate or mixed solutions with the SiO_2:Na_2O molar ratio from 1.00 to 3.22, by different methods such as immersion or electrolytic deposition. Aramaki [7] found that sodium silicate ($Na_2Si_2O_5$) is remarkably effective on zinc corrosion, exhibiting high inhibition efficiencies around 90%. Some results are also drawn that silicate sodium can enclose the pores of zinc phosphate film [14] and help to increase the self-healing of some coatings [15–17]. Parashar et al. [19] have reported that the properties of the silicate coatings (the drying rate and chemical resistance properties) are directly proportional to the ratio of silica to alkali metal oxide. But, very few works are reported on the relationship between the properties of single silicate coating and SiO_2:Na_2O molar ratio of sodium silicate solution.

In this paper, the relationship between the properties of the silicate coatings formed on HDG samples and the SiO_2:Na_2O molar ratio of sodium silicate solution was systematically investigated. The corrosion resistance of silicate coatings was evaluated by means of Tafel polarization, electrochemical impedance spectroscopy (EIS) measurements and neutral salt spray (NSS) test. The morphology of silicate coatings was investigated by scanning electron microscopy (SEM) and atomic force microscopy (AFM). The chemical composition of the layer was investigated in this paper mainly by X-ray photoelectron spectroscopy (XPS), X-ray diffraction analysis (XRD) and reflectance absorption infrared spectroscopy (RA-IR) for a SiO_2:Na_2O molar ratio of 3.50.

* Corresponding author. Tel./fax: +86 20 85511540.
E-mail address: konggang@scut.edu.cn (G. Kong).

0257-8972/$ – see front matter © 2009 Elsevier B.V. All rights reserved.
doi:10.1016/j.surfcoat.2009.10.024

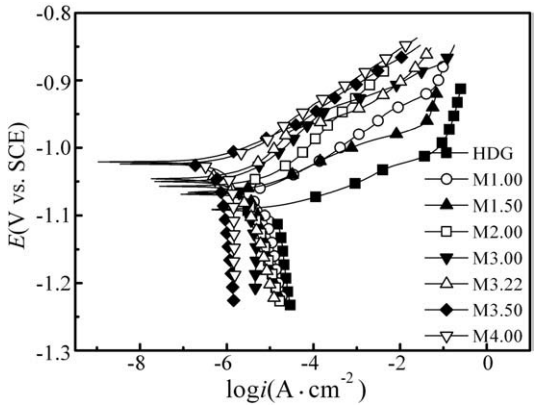

Fig. 1. Tafel polarization curves for the HDG sample and the M*X* coatings immersed in 5% NaCl solution.

2. Experimental

Sodium silicate solution with 5 wt.% SiO_2 in this study was used as the silicate precursor. The effect of the SiO_2:Na_2O molar ratio was studied by varying the SiO_2:Na_2O molar ratio of sodium silicate solution with 5 wt.% SiO_2. Studies were performed in 1.00, 1.50, 2.00, 3.00, 3.22, 3.50 and 4.00. For example, 250 g sodium silicate with the SiO_2:Na_2O molar ratio of 3.50 can be prepared by adding 12.50 g SiO_2 and 4.75 g NaOH to 233.42 ml de-ionized water.

The substrate that consisted of HDG steel (zinc layer thickness of approximately 50 μm) was prepared using the following process. Q235 cold rolled steel sheets of 50 mm × 40 mm × 2 mm were degreased, pickled, fluxed in a mixed solution with 150 g/l NH_4Cl and 100 g/l $ZnCl_2$ at 60 °C, dried and dipped in zinc bath at 450 °C for 1 min, and then withdrawn slowly and quenched in water immediately. Prior to immersion, the freshly HDG samples were rinsed with ethanol and de-ionized water. Immersion was done at ambient temperature for 1 min. After immersion, the silicate-treated HDG samples were then dried at 100 ± 5 °C for 20 min. The symbol M*X* is used to sign the samples treated by different processes. The number "*X*" behind "M" is the SiO_2:Na_2O molar ratio of the sodium silicate solution and HDG denotes the untreated HDG sample.

Tafel polarization and electrochemical impedance spectroscopy (EIS) measurements were used to evaluate the corrosion resistance of the silicate coatings and HDG during immersion in a non-deaerated 5 wt.% sodium chloride solution, at room temperature. The measurements were performed in a three-electrode system using a potentiostat/galvanostat response analyzer of electrochemical workstation (Model: CHI 604B). A saturated calomel electrode (SCE), connected to the 5 wt.% NaCl solution through a Luggin capillary, was used as a reference, a platinum foil as the auxiliary electrode, and the samples as the working electrode with the exposed area of 1.00 cm^2. EIS measurements were carried out at corrosion potential in a frequency range between 100 kHz and 10 mHz with a potential sine signal of 10 mV. The scan rate for polarization was 1 mV/s. The EIS data of silicate coatings are evaluated using the ZView (version 2.1C) software.

Table 1
Electrochemical parameters obtained from Fig. 1.

Sample ID	R_p/(kΩ cm^2)	E_{cor}/V vs. SCE	i_{cor}/(μA cm^{-2})
HDG	0.49	−1.09	12.50
M1.00	1.95	−1.07	4.13
M1.50	2.34	−1.07	3.32
M2.00	3.37	−1.06	2.51
M3.00	6.28	−1.05	1.41
M3.22	9.15	−1.05	0.84
M3.50	20.97	−1.02	0.34
M4.00	11.91	−1.03	0.68

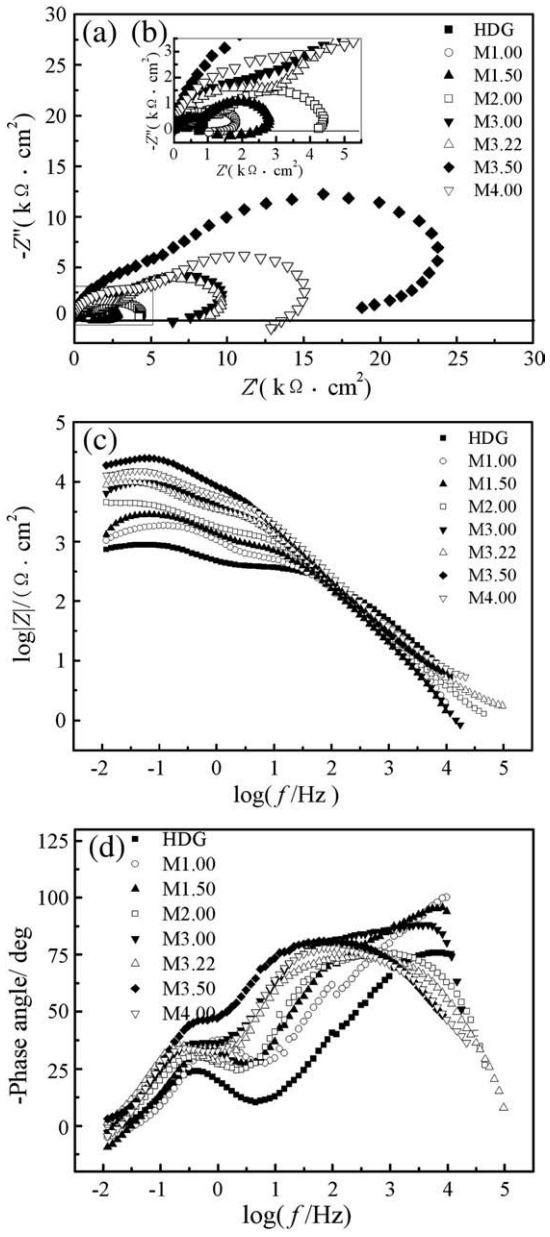

Fig. 2. Nyquist and Bode diagrams for the HDG sample and the M*X* coatings immersed in 5% NaCl solution, including (b) local amplification.

Corrosion resistance was also evaluated by neutral salt spray (NSS) test carried out in the NSS chamber (Model: YWX/Q150) and conducted using a 5 wt.% NaCl solution with pH 6.50–7.00 at (35 ± 2) °C. The samples were placed perpendicularly with an angle of 30°. Each sample was sprayed for 8 h, and then kept in the NSS chamber for 16 h, defined as a spray cycle. The corroded area was measured by grid method after a certain spray time (or cycle) to evaluate the corrosion resistance.

The morphology of the coatings was observed using scanning electron microscopy (SEM) (GERMAN LEO; Model: LEO 1530 vp) and atomic force

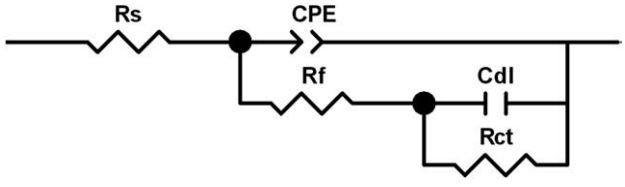

Fig. 3. Electrical circuit used to fit the EIS results.

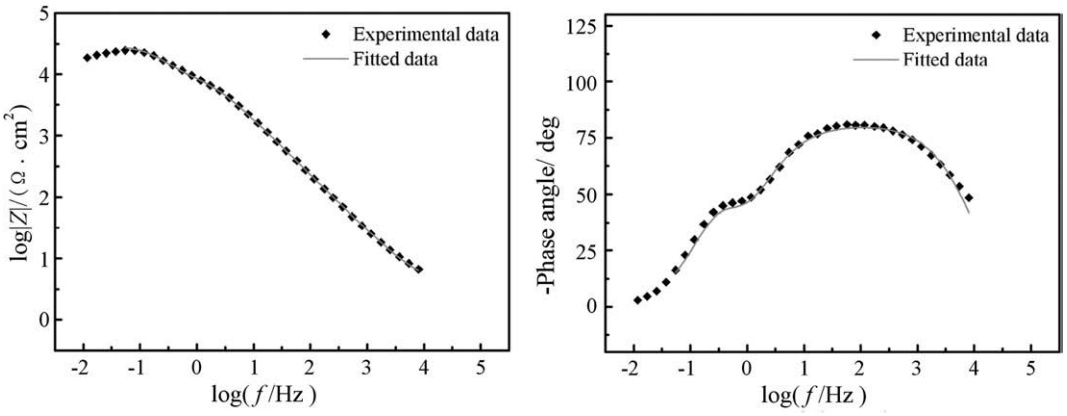

Fig. 4. Bode diagrams of the experimental and fitted impedance spectra (the surface of the silicate coating on M3.50).

microscopy (AFM) (JAPAN SEIKO; Model: SPI3800N). The chemical composition of surface and depth analysis of the coatings was analyzed using X-ray photoelectron spectroscopy (XPS) (Model: AXIS ULTRA^{DLD}). The coatings were also investigated by X-ray diffraction analysis (XRD) (JAPAN RIGAKU; Model: Dmax/IIIA) with Cu-Kα target and reflectance absorption infrared spectroscopy (RA-IR) (GERMAN BRUKER; Model: Vector 33).

3. Results and discussion

3.1. Corrosion resistance of the silicate coatings

3.1.1. Tafel polarization curves

Tafel polarization curves for HDG and M*X* are shown in Fig. 1, and the corresponding electrochemical parameters obtained from the Tafel polarization curves are listed in Table 1. It can be seen that both the anodic and cathodic branches of the polarization curves for M*X* are shifted towards the direction where the corrosion current densities (i_{cor}) decreased, indicating that the anodic process ($Zn \rightarrow Zn^{2+} + 2\,e^-$) and cathodic process ($O_2 + 2\,H_2O + 4\,e^- \rightarrow 4\,OH^-$) of zinc corrosion are inhibited simultaneously. The i_{cor} values of all M*X* are lower than that of HDG, and they are decreased with increasing of the SiO_2:Na_2O molar ratio in the range from 1.00 to 3.50. Correspondingly, the polarization resistance (R_p) has an opposite change to the i_{cor}. The i_{cor} value of M3.50 is minimal, about 0.34 μA cm^{-2} and the R_p value of M3.50 is also maximal, about 20.97 kΩ cm^2.

3.1.2. EIS measurements

The Nyquist and Bode diagrams for HDG and M*X* immersed in 5 wt.% NaCl are shown in Fig. 2. The total impedance values of all M*X* are higher than that of HDG. This may be due to the surface of zinc layer of M*X* that is covered by the silicate coatings. The total impedance values of M*X* increase with increasing the SiO_2:Na_2O molar ratio in the range from 1.00 to 3.50 but decrease for a higher molar ratio. For example, the total impedance value of M1.00 and M4.00 is separately about 1.82 kΩ cm^2 and 15.05 kΩ cm^2, while that of M3.50 is about 23.77 kΩ cm^2. This is in a good agreement with the results of Tafel polarization. It further indicates that the corrosion resistance of the HDG steels is enhanced by sodium silicate treatment.

Silicate coatings formed on HDG could be also described by equivalent electrical circuit presented in Fig. 3. Due to the complexity of the systems and uncertainty of inductive model theories, this equivalent circuit only represents a simplified manner to describe the electrochemical interface excluding inductive loops, and a fitting result in Fig. 4 made by this model proved our hypothesis. In this circuit R_s corresponds to the solution resistance; the constant phase element (CPE) is related with the double layer capacity of the solution/coating interface in the range of high and intermediate frequencies, which substitutes the "ideal" capacitance in view of the heterogeneous and/or porous/rough nature of the electrode in electrochemical process [20–22], R_f delegates the charge transfer resistance processes occurring within the pores of coating and on the surface; R_{ct} and C_{dl} represent the resistance and the capacitance of HDG substrate/coating interface responded at low frequency. The HDG substrate/coating interface is due to the interaction of Zn–OH groups with Si–OH, forming Zn–O–Si bond [1]. The results of the fitting procedure are presented in Table 2.

As shown in Table 2, HDG without treatment shows the lowest resistance and highest capacitance, indicating that SiO_2:Na_2O molar ratio of sodium silicate solution promotes the formation of more anticorrosive silicate coatings on HDG surfaces. The R_f values of M*X* increase with increasing the SiO_2:Na_2O molar ratio in the range from 1.00 to 3.50 but decrease for a higher molar ratio, which indicates that different changes in the electrode/electrolyte interface happened during immersion. However, the Y_0 and n values of silicate coatings are not in good accordance with linear law, because of the existence of pinholes or defects in silicate coatings and difference of roughness of silicate coatings surfaces.

Because the damage of this interface facilitates electrolyte species' enter into the HDG substrate [23,24], and R_{ct} delegates more faithfully

Table 2
Values of the elements related to HDG and the silicate coatings, determined from the fit to the mode of Fig. 3.

Sample ID	R_s/(Ω cm^2)	R_f/(kΩ cm^2)	Y_0(CPE-T)/10^{-5} (Ω^{-1} cm^{-2} s^{-n})	n(CPE-P)	R_{ct}/(kΩ cm^2)	C_{dl}/10^{-5} (F cm^{-2})
HDG	0.96	0.40	2.02	0.80	0.52	100.64
M1.00	1.16	0.57	1.77	0.89	1.38	19.64
M1.50	0.51	0.93	1.44	0.94	1.93	21.10
M2.00	1.04	1.61	1.74	0.88	2.80	26.34
M3.00	0.32	3.59	1.14	0.97	6.87	9.55
M3.22	1.71	3.97	1.94	0.85	6.69	19.31
M3.50	4.10	11.96	1.24	0.91	17.37	4.13
M4.00	4.04	7.04	1.29	0.87	10.14	10.73

Surface of the working electrode: 1 cm^2.

Table 3
Results of neutral salt spray test (corrosion area ratio, pct).

Sample ID	2 h	4 h	6 h	8 h	1 cycle	2 cycles	3 cycles	4 cycles
HDG	30	50	65	75	80	87	98	98
M1.00	0	1	3	3	6	10	15	20
M1.50	0	0	2	3	5	8	12	18
M2.00	0	0	0	0	1	4	10	15
M3.00	0	0	0	0	0	3	5	10
M3.22	0	0	0	0	0	2	4	8
M3.50	0	0	0	0	0	0	2	5
M4.00	0	0	0	0	0	2	3	7

the corrosion resistance of the coated substrate [22], it is better to focus in R_{ct} values for this EIS fitting results analysis. The R_{ct} values of HDG and silicate coatings are in good accordance with R_p. The R_{ct} value of M3.50 is remarkably higher than those of HDG and other silicate-treated samples, which may be due to the formation of a most compact interface layer in the silicate solution with SiO_2:Na_2O molar ratio of 3.50. Moreover, one high frequency (HF) inductive loop appears in the EIS diagrams for HDG and M*X* (except M3.50), as shown in Fig. 2. This can be deduced that the water permeates into the coatings through pinholes or other defects, because the LF inductive loop is attributed to the dissolution of zinc [14,25,26].

This further indicates that the transfer of the charge is hindered and the diffusion of the electrolyte in the pores of the coatings is blocked to the extent by silicate coatings conspicuously in comparison to HDG. Moreover, the dissolution of zinc is suppressed by silicate coatings when the SiO_2:Na_2O molar ratio is 3.50.

3.1.3. Neutral salt spray test

Table 3 presents the NSS results of HDG and M*X*. In accordance with the previously discussed results, it can be observed that increasing the SiO_2:Na_2O molar ratio, up to 3.50, decreases the corroded area, indicating better corrosion resistance. Moreover, M4.00 exhibited lower protective performance than M3.50 on which no corrosion products is observed in two spray cycles. Therefore, these data confirm the positive effect on corrosion protection for the HDG steels, of the sodium silicate solution with SiO_2:Na_2O molar ratio in the range from 1.00 to 4.00, especially 3.50.

According to Iler [27] and Veeraraghavan et al. [1], $Si(OH)_4$ (monomer, Q_0 type), which bears OH group, can be condensed on zinc surface (namely ZnOH bond), leading to the formation of silicate on zinc surface at a specified pH value. Usually, when the SiO_2:Na_2O molar ratio of a sodium silicate solution is over 2.00, a part of the silicate can condense to polymeric silica, forming silica sol [28]. The amount of polymeric silica containing Si–OH groups is proportional to the SiO_2:Na_2O molar ratio of silicate solutions. The higher the molar ratio is, the more the silica and the polymeric silica will be formed in the solution. Conversely, the lower the molar ratio is, the more monomeric silica and the higher pH value are in the solution. At a certain range of pH values, a certain amount of polymeric silica is beneficial to form a continuous coating. However, the zinc hydroxide may be dissolved for an overhigh pH value, and polymeric silica may be over-polymerized for an overmuch silica [29,30], resulting in a detrimental effect on the formation of the silicate coatings.

3.2. Morphology of the silicate coatings

The SEM technique was used to examine the surface morphology of the silicate coatings on M*X*. From M1.00 to M4.00, the appearance of the silicate coatings is bright and shiny, similar to that of zinc layer, as we can see with the representative image in Fig. 5. The zinc grains below the silicate coating can still be observed, showing that the silicate coating is thin and transparent, and there is no bubble, peeling and shelling.

Fig. 6 shows two-dimensional AFM images of M1.00, M2.00, M3.50, and M4.00 obtained for a scanned area of 5 μm × 5 μm. It can be seen that surface morphology of different coatings differs from each other. M1.00 coating shows appearance of pinholes, pores, and large nodules on the surface (Fig. 6a). With the increase in the SiO_2:Na_2O molar ratio of silicate solutions the tendency of appearance of pinholes/pores and the rms roughness for coatings decreases, as we can see with the representative images in Fig. 6b and c. Moreover, the surface appears to have a more fine-grained structure. For a higher molar ratio, the rms roughness for silicate coating increases, as shown in Fig. 6d. Therefore, the corrosion resistance of silicate coatings is increased, charge transfer and electrolyte diffusion are further blocked with increasing SiO_2:Na_2O molar ratio of the silicate solution in the range from 1.00 to 3.50, but decrease for a higher molar ratio. In the next section, the chemical composition and structure of the silicate coatings on M3.50 will be further discussed as the representative result, because of no obvious differences of those in various silicate coatings.

3.3. Chemical composition and structure of the silicate coatings

Fig. 7 shows the XPS spectrum of the silicate coating on M3.50. The surface of coating mainly contains the elements of Zn, Si, O, Na and C. The element of C might be due to the environmental contamination, and the element of Na may be due to the residual sodium silicate solution on the sample which was not rinsed after taking out of the solution.

Fig. 8 shows the high resolution XPS spectra of Zn 2p, Si 2p, O 1s, and Na 1s. As shown in Fig. 8a, the peak of Zn 2p at 1021.60 eV is close to that reported for Zn^{2+} $2p_{3/2}$ in zinc silicate and zinc oxide/hydroxide [15], while the other peak at 1044.50 eV corresponds to Zn $2p_{1/2}$ [31]. As shown in Fig. 8b, the peak of Si 2p at 102.90 eV corresponds to silicate and silica [31,32]. As shown in Fig. 8c, the O 1s peak can be resolved into three peaks with the binding energies of 531.92 eV, 532.22 eV and 532.82 eV. They correspond to zinc silicate, zinc hydroxide and silica respectively. The peak of Na 1s at 1071.40 eV corresponds to Na(I) (in Fig. 8d).

Table 4 shows the chemical composition of the silicate coating on M3.50 as a function of sputtering time by means of XPS profile depth analyses. The results show that the Na and C elements disappear after a short sputtering time (45 s). The coating is mainly composed of the elements of Zn, O, and Si. Furthermore, the Zn content is increased and the O/Si ratio is gradually decreased with increasing sputtering time, which may result in the gradual increasing of ZnO and the gradual decreasing of SiO_2 from surface to inner. The silicate coating contains Zn element, suggesting that Zn participates in coating formation reaction.

In the XRD pattern of the silicate coatings (not listed in this paper), many disorderly small peaks appear. So it is difficult to identify the

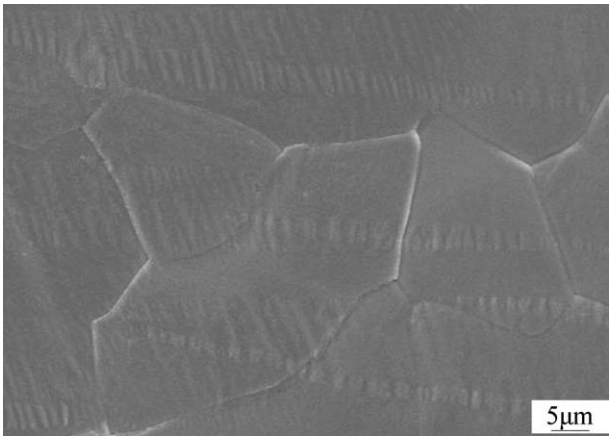

Fig. 5. SEM micrograph of the silicate coating on M3.50.

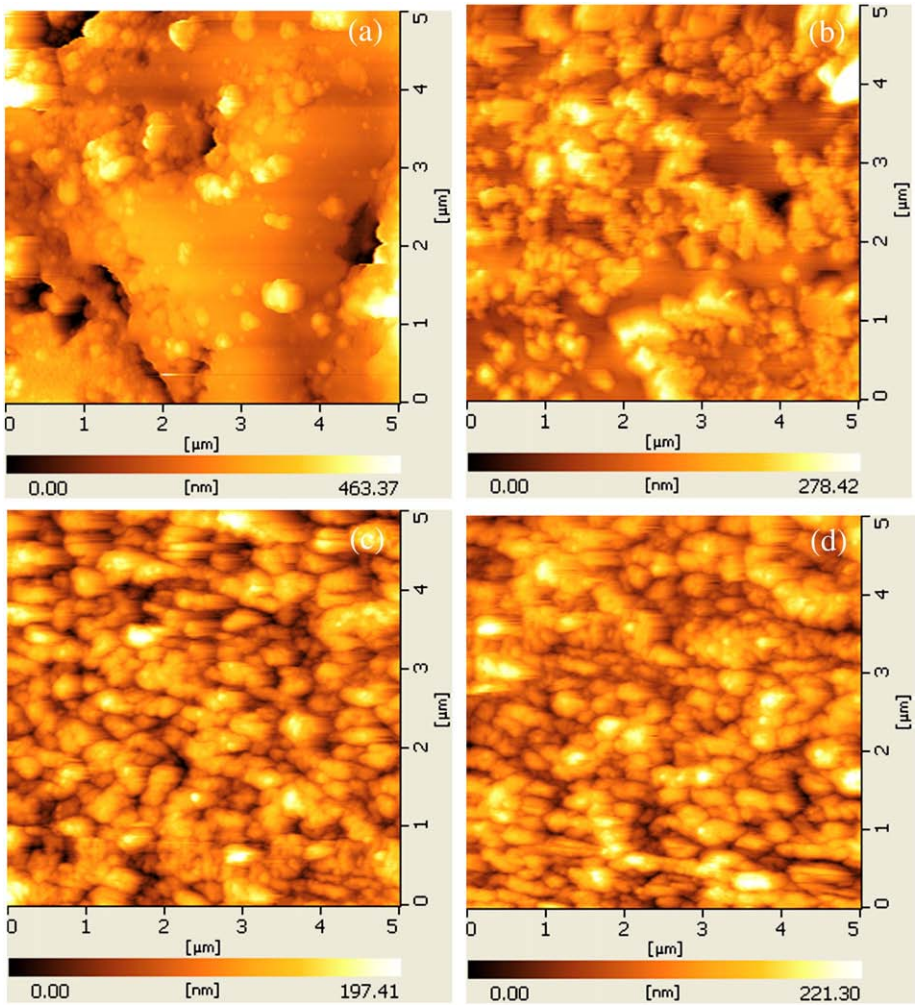

Fig. 6. AFM images of the silicate coatings (a) M1.00, (b) M2.00, (c) M3.50, and (d) M4.00.

phases exactly. But it can be affirmed that there exist the SiO_2 phase for a distinct peak at $2\theta = 9.15$.

Fig. 9 shows the RA-IR spectrum of the silicate coating on M3.50. The peaks in the region between 3483 cm^{-1} and 3000 cm^{-1} are assigned to the –OH stretching vibration band; the peak at 1224 cm^{-1} is assigned to the Si–O–Si bond [33]; the peak at 1017 cm^{-1} is probably assigned to the Si–O–Zn bond [34,35].

Based on the above results, the silicate coating on M3.50 may be mainly composed of zinc oxides/hydroxides, zinc silicate and SiO_2, and is a chemical conversion coating. Hence, it can be deduced that the process of forming a silicate coating from inside to the outside proceeds as follows [1,19,27]. The Zn–OH groups on the surface react with silicate ions and polymeric silica to form an extensively cross-linked or dense inner layer dominated with Si–O–Si and Zn–O–Si bonds; redundant polymeric silica condenses to form an outer layer of polymeric silicate with Si–O–Si bonds. Then dehydrates and finally forms a silicate conversion coating on the surface of HDG steel. In a corrosive environment, the silicate coating acts as a physical barrier to inhibit the transfer of the charges and the movement of the ions. Consequently, the electrochemical corrosion of the zinc layer is restrained.

4. Conclusions

In this paper, a transparent silicate coating was prepared by immersing HDG steel in sodium silicate solution with a SiO_2:Na_2O molar ratio. The influence of the SiO_2:Na_2O molar ratio of silicate solution on the properties of silicate coatings was investigated. The results of the electrochemical tests show that in comparison to HDG, the corrosion current densities of silicate coatings are decreased, the polarization resistance and the total impedance values are increased markedly, and the corrosion resistance is enhanced. The protective performance of the silicate coating is constantly enhanced with the SiO_2:Na_2O molar ratio up to 3.50 but decreased for a higher molar ratio. The corrosion resistance of the sample is optimal when the SiO_2:Na_2O molar ratio of silicate solution was 3.50. The silicate

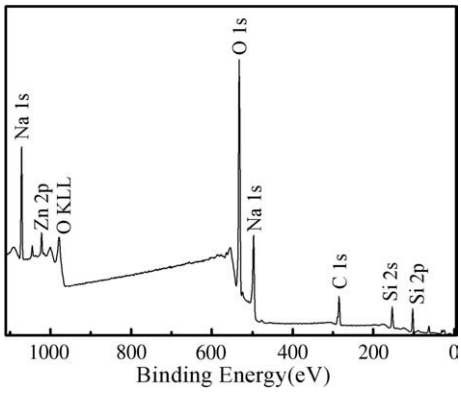

Fig. 7. XPS spectrum of the surface of the silicate coating on M3.50.

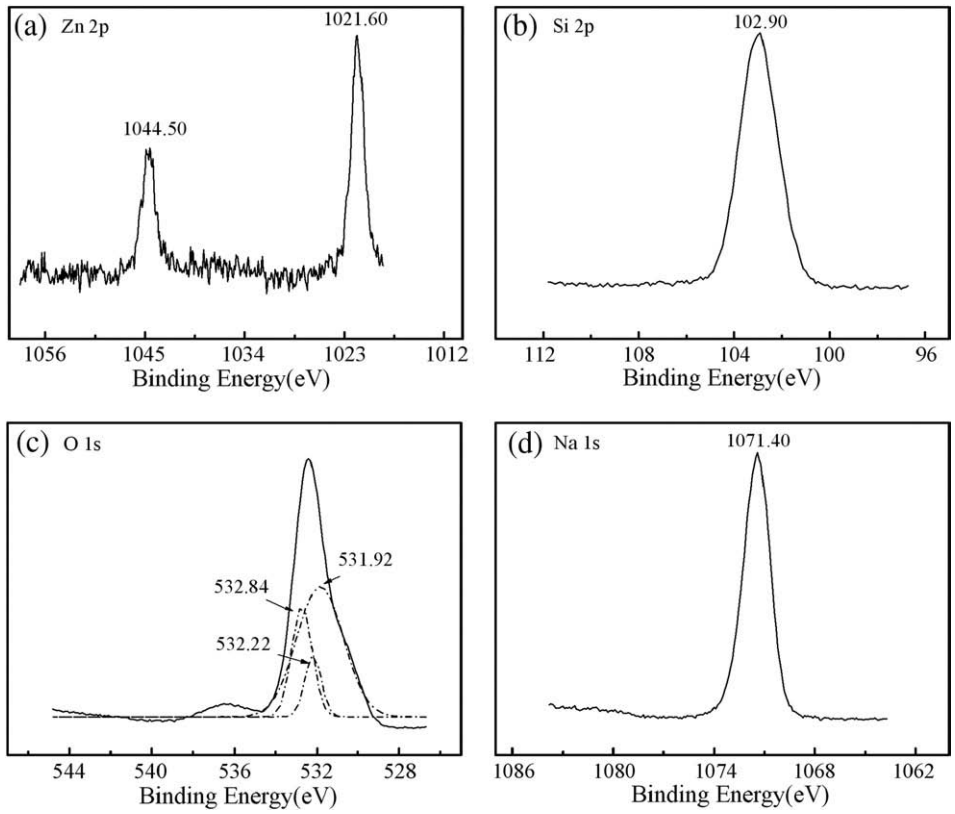

Fig. 8. High resolution XPS spectra of Zn 2p (a), Si 2p (b), O 1s (c) and Na 1s (d) for the surface of the silicate coating on M3.50.

Table 4
Data of XPS depth analyses of the silicate coating on M3.50.

Etching time/seconds	Zn/atomic, pct	O/atomic, pct	Si/atomic, pct	O/Si
45	0.46	70.04	29.50	2.37
180	0.47	68.99	30.54	2.26
270	0.99	68.77	30.24	2.27
360	2.15	67.48	30.37	2.22
720	8.35	62.50	29.15	2.14
1260	13.35	58.68	27.97	2.10
1800	20.04	52.32	27.64	1.89

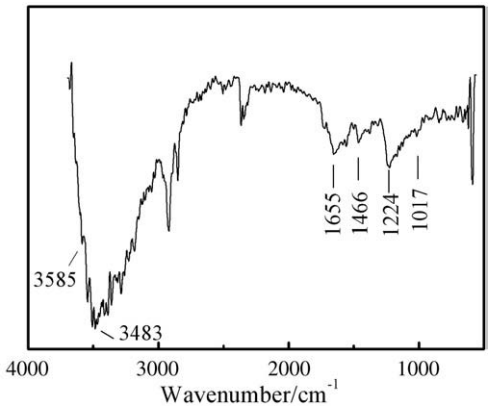

Fig. 9. RA-IR spectrum of the silicate coating on M3.50.

coatings mainly are composed of zinc oxides/hydroxides, zinc silicate and SiO_2. It is considered that the coatings may be a kind of network structure with cross-linked Si–O–Si and Si–O–Zn bonds. Additionally, it is found that the morphology of silicate coatings is different by AFM images, which is responsible for the corrosion resistance of silicate coatings.

References

[1] B. Veeraraghavan, D. Slavkov, S. Prabhu, M. Nicholson, B. Haran, B. Popov, B. Heimann, Surf. Coat. Technol. 167 (2003) 41.
[2] J.H. Osborne, Prog. Org. Coat. 41 (2001) 280.
[3] B.L. Lin, J.T. Lu, G. Kong, J. Liu, Trans. Nonferr. Met. Soc. China 17 (2007) 755.
[4] D.E. Walker, G.D. Wilcox, Trans. Inst. Met. Finish. 86 (2008) 251.
[5] V.S. Gireesh, S.M.A. Shibli, Corros. Prev. Control. 48 (2001) 11.
[6] J.T. Lu, H.J. Wu, G. Kong, C.S. Che, Q.Y. Xu, Trans. Nonferr. Met. Soc. China 16 (2006) 1397.
[7] K. Aramaki, Corr. Sci. 43 (2001) 591.
[8] J.B. Bajat, Z. Kačarević-Popović, V.B. Mišković-Stanković, M.D. Maksimović, Prog. Org. Coat. 39 (2000) 127.
[9] R.M. Souto, V. Fox, M.M. Laz, S. Gonzalez, J. Adhes. Sci. Technol. 14 (2000) 1321.
[10] P. Roose, I. Fallais, C. Vandermiers, M.-G. Olivier, M. Poelman, Prog. Org. Coat. 64 (2009) 163.
[11] M.F. Montemor, A. Rosqvist, H. Fagerholm, M.G.S. Ferreira, Prog. Org. Coat. 51 (2004) 188.
[12] P. Nemeth, A. Csanady, K. Papp, A.Cs Pinter, L. Szabo, Z. Paszti, A. Toth, E. Kalman, Mater. Sci. Forum. 589 (2008) 433.
[13] J.J. Hahn, N.G. McGowan, R.L. Heimann, T.L. Barr, Surf. Coat. Technol. 108–109 (1998) 403.
[14] B.L. Lin, J.T. Lu, G. Kong, Surf. Coat. Technol. 202 (2008) 1831.
[15] K. Aramaki, Corr. Sci. 44 (2002) 1621.
[16] K. Aramaki, Corr. Sci. 44 (2002) 1375.
[17] A.S. Hamdy, Surf. Coat. Technol. 200 (2006) 3786.
[18] X.C. Shi, G. Jarjoura, G.J. Kipouros, Magnes. Technol. 2006 (2006) 273.
[19] G. Parashar, M. Bajpayee, P.K. Kamani, Surf. Coat. Int. Part B Coat. Trans. 86 (2003) 209.
[20] Z.P. Yao, Z.H. Jiang, F.P. Wang, Electrochim. Acta 52 (2007) 4539.
[21] Y.S. Bao, W. Wang, B.L. He, M. Wang, Y.S. Yin, L. Liang, L. Xu, G.C. Xu, Electrochim. Acta 54 (2008) 611.

[22] P.H. Suegama, H.G. de Melo, A.A.C. Recco, A.P. Tschiptschin, I.V. Aoki, Surf. Coat. Technol. 202 (2008) 2850.
[23] M.L. Zheludkevich, R. Serra, M.F. Montermor, K.A. Yasakau, I.M.M. Salvado, M.G.S. Ferreira, Electrochim. Acta 51 (2005) 208.
[24] M. Quinet, B. Neveu, V. Moutarlier, P. Audebert, L. Ricq, Prog. Org. Coat. 58 (2007) 46.
[25] C. Cachet, F. Ganne, G. Maurin, J. Petitjean, V. Vivier, R. Wiart, Electrochim. Acta 47 (2001) 509.
[26] C. Cachet, F. Ganne, S. Joiret, G. Maurin, J. Petitjean, V. Vivier, R. Wiart, Electrochim. Acta 47 (2002) 3409.
[27] R.K. Iler, The Chemistry of Silica: Solubility, Polymerization, Colloid and Surface Properties and Biochemistry, John Wiley & Sons, New York, 1979.
[28] J.L. Bass, G.L. Turner, J. Phys. Chem. B. 101 (1997) 10638.
[29] I.L. Svensson, S. Sjöberg, L.-O. Öhman, J. Chem. Soc. Faraday Trans. 82 (1986) 3635.
[30] S. Sjöberg, J. Non-Cryst. Solids. 196 (1996) 51.
[31] J.Q. Wang, W.H. Wu, W.M. Feng, XPS/XAES/UPS, National Defense Industry Press, Beijing, 1992 (in Chinese).
[32] K. Aramaki, Corr. Sci. 44 (2002) 871.
[33] M. Hara, R. Ichino, M. Okido, N. Wada, Surf. Coat. Technol. 169–170 (2003) 679.
[34] M.A. Chen, X. Xie, H.Y. Qi, X.M. Zhang, H.Z. Li, X. Yang, W.L. Huaxue Xuebao, Acta Phys.-Chim. Sin. 22 (2006) 1025 (in Chinese).
[35] H. Kim, J. Jang, J. Appl. Polym. Sci. 68 (1998) 785.